bonyl compounds show this effect as well: for a series of ring-substituted 3-benzylpentane-2,4-diones, $\alpha = 0.77$ while $\beta = 0.44$.[50]

Now consider variations in the R_1 group of eq 26. This group is more remote than R_2 from the central carbon on which negative charge builds up in the transition state, but it is closer than R_2 to the enolate oxygen atom where the charge is relocated in the final state. Lagging charge relocation will therefore cause R_1 to have less of an effect on the rate constant than expected from its effect on the equilibrium constant and the magnitude of β. The result will be a diminished value of α, as is observed.

Another manifestation of transition-state imbalance may be obtained by comparing rate and equilibrium constants for the ionization of acetaldehyde determined here with those for isobutyraldehyde.[6] Isobutyraldehyde is the stronger acid, $pK_a^K = 15.49$ as opposed to $pK_a^K = 16.73$ for acetaldehyde, and yet the specific rate for proton transfer from isobutyraldehyde to hydroxide ion, $k = 0.142\ M^{-1}\ s^{-1}$, is less than that for the same reaction of acetaldehyde, $k = 1.17\ M^{-1}\ s^{-1}$. These data give the "abnormal" Brønsted exponent $\alpha = -0.3$.[51]

A similar situation is found for the ionization of the analogous nitro compounds, nitromethane and 2-nitropropane, where $\alpha = -0.5$.[49b] This phenomenon has also been attributed to lagging negative charge relocation in the transition state, which exalts the effect of methyl substitution on the reaction rate, but this time the effect is coupled with methyl-group stabilization of the carbon-nitrogen double bond of the nitronate ion.

A similar explanation may be advanced for the case of acetaldehyde and isobutyraldehyde. Methyl-group stabilization of the carbon-carbon double bond dominates in the final state enolate ion because the methyl groups are now remote from the relocated negative charge; isobutyraldehyde is thus a stronger acid than acetaldehyde. In the transition state, on the other hand, the not yet delocalized negative charge is near the site of methyl substitution and the destabilizing, electron-supplying polar effect of methyl dominates. The effects of methyl substitution upon rate and equilibrium constants are thus in opposite directions, and a negative value of α results.

Acknowledgment. We are grateful to the Natural Sciences and Engineering Research Council of Canada, the donors of the Petroleum Research Fund, administered by the American Chemical Society, the Swiss National Science Foundation, and the Ciba Stiftung for their financial support of this work.

Supplementary Material Available: Tables S1-9 of rate data (10 pages). Ordering information is given on any current masthead page.

(50) Bell, R. P.; Grainger, S. *J. Chem. Soc., Perkin Trans. 2* **1976**, 1367-1370.

(51) Statistical factors $p = 3$ and $q = 1$ for CH_3CHO and $p = 1$ and $q = 1$ for $(CH_3)CHCHO$ were used in this calculation.

Experimental and Theoretical Evidence for Nonlinear Coordination of "sp-Hybridized" Carbon Atoms: The Gas-Phase Structure of Trifluoroethylidynesulfur Trifluoride, $CF_3—C{\equiv}SF_3$

Dines Christen,[1a] Hans-Georg Mack,[1a] Colin J. Marsden,*[1d] Heinz Oberhammer,*[1a] Gabriele Schatte,[1b] Konrad Seppelt,[1c] and Helge Willner[1b]

Contribution from the Institut für Physikalische und Theoretische Chemie, Universität Tübingen, 7400 Tübingen, West Germany, Institut für Anorganische Chemie, Universität Hannover, 3000 Hannover, West Germany, Institut für Anorganische und Analytische Chemie, Freie Universität Berlin, 1000 Berlin, West Germany, and Department of Inorganic Chemistry, University of Melbourne, Parkville, Victoria 3052, Australia. *Received October 9, 1986*

Abstract: We report an extensive series of studies, both experimental and theoretical, which probe the shape of CF_3CSF_3 and its skeletal bending potential. Gas phase and matrix IR and Raman spectra have been recorded and assigned, and a force field has been obtained. The vibrational assignment is most simply based on a C_{3v} model with a linear C—C≡S skeleton, but small deviations from linearity cannot be excluded. The gas-phase molecular structure has been studied by electron diffraction. A range of molecular models has been considered, including the effects of internal rotation of the CF_3 group and of large-amplitude bending at the two-coordinate carbon. A linear skeleton is incompatible with the diffraction data. The barrier to linearity is greater than 2 kJ mol^{-1} but cannot be determined precisely. The average C—C≡S angle is 155 (3)° (3σ uncertainties in parentheses) for all acceptable models; this is a substantially greater deviation from linearity than found in solid CF_3CSF_3. The electron diffraction model is supported by broad band microwave spectroscopy, which yields B + C = 1.545 GHz in very good agreement with the structure derived by electron diffraction. Other geometrical parameters (r_a values) are C—F = 1.329 (4) Å, C—C = 1.45 (2) Å, S≡C = 1.434 (14) Å, S—F = 1.561 (3) Å, FCF = 108.4 (5)°, and FSF = 93.2 (9)°. Ab initio calculations have been performed for $HC{\equiv}SF_3$, $FC{\equiv}SF_3$, $CH_3C{\equiv}SF_3$, and $CF_3C{\equiv}SF_3$. All are linear at carbon with use of SCF wave functions but are predicted to bend, though to very different extents, when electron correlation is included at the MP2 level. Calculations on $HC{\equiv}SH_3$ showed that the MP2 method *underestimates* the influence of electron correlation on the skeletal bending potential.

The first compound containing a C≡S triple bond has recently been prepared,[2,3] and its geometric structure has attracted some interest by theoreticians and experimentalists. Ab initio calculations in the HF approximation[4] and a low-temperature X-ray study[3] result in very short C≡S (1.404 and 1.420 (5) Å, respectively) and C—C bonds (1.439 and 1.434 (7) Å) and in FSF angles near 90° (92.7° and 90.9°-94.3°). These studies differ, however, with respect to the configuration of the C—C≡S

(1) (a) Tübingen. (b) Hannover. (c) Berlin. (d) Melbourne.

(2) Pötter, B.; Seppelt, K. *Angew. Chem.* **1984**, *96*, 138.

(3) Pötter, B.; Seppelt, K.; Simon, A.; Peters, E. M.; Hettich, B. *J. Am. Chem. Soc.* **1985**, *107*, 980.

(4) Boggs, J. E. *Inorg. Chem.* **1984**, *23*, 3577.

0002-7863/87/1509-4009$01.50/0

Table I. Experimental Vibrational Frequencies for CF_3CSF_3 (cm^{-1})[a]

IR gas	Ne matrix	Ar matrix	Raman	assignment
2444 vw				
2386 vw				
2315 w				
2150 vw				
2087 w				
2029 vw				
1800 vs (sh) br	1810[b]	1795[b]	1770 w, br	$\nu_1 a_1$
1742 vs, br				
1450 vw				
1320 vw				
1225 vw				
1225 s PQR (8)	1224 [33]	1223	1220 w	$\nu_2 a_1$
1167 vs	1164 [33]	1155	1150 w, br	$\nu_8 e$
1059 vw				
863 vs	860	859		$\nu_9 e$
795 vs	795[b]	800[b]	785 w, br	$\nu_3 a_1$
728 s PQR (8)	728	727	724 vs	$\nu_4 a_1$
640 vw				
590 w (sh)	590	588	583 w	$\nu_{10} e$
569 m PQR (8)	568	570	569 s	$\nu_5 a_1$
540 w				
505 w				
			433 m	$\nu_{11} e$
402 m-w, br	403	03	402 m	$\nu_{12} e$
330 m-w PQR (8)	329	330	328 s	$\nu_6 a_1$
271 w	275	277	274 vs	$\nu_{13} e$
229 vw			199 vw	$^2\nu_{14}$

[a] Values in ( ) = $\Delta\nu$(PR), [ ] = $^{12/13}C$ isotope shifts. [b] Split due to matrix effects.

skeleton. Whereas the calculations predict a linear chain, the X-ray study results in a slightly bent configuration with C—C≡S = 171.5 (20)°.

It is difficult to assess whether, and to what extent, crystal packing forces might distort the structure of CF_3CSF_3, but a qualitative analysis of the packing makes it unlikely that this small deviation from linearity is due to such packing effects.[3] Since nonlinear coordination at a formally sp-hybridized carbon is unexpected and would violate a fundamental rule of elementary valence theory, we thought it desirable to examine the shape of the C—C≡S skeleton in more detail, by studying the free molecule in the gas phase. In this article we report a gas electron diffraction as well as broad band microwave spectroscopy study and analysis of gas, liquid, and matrix vibrational spectra. We have also performed ab initio calculations on $HCSF_3$, $FCSF_3$, CH_3CSF_3, and CF_3CSF_3 to probe the bending potentials of $XC{\equiv}SF_3$ systems. We were able to include the effects of electron correlation in these calculations, and we show that, most unusually, they qualitatively change the predicted shape of these $XC{\equiv}SF_3$ molecules.

As our work was being prepared for publication, another ab initio study of CF_3CSF_3 was reported by Dixon and Smart.[5] They optimized the structure, predicted vibrational frequencies at the SCF level, and surveyed the influence of electron correlation on the shape of the C—C≡S skeleton. Their conclusions are not consistent with our experimental results.

Experimental Section

Sample. The compound was prepared as described in the literature[1,2] and purified by repeated fractional condensation. The purity was checked by NMR spectroscopy.

Vibrational Spectra. Gas-phase IR spectra were recorded in the range 4000–100 cm^{-1} with a resolution of 4, 1, and 0.1 cm^{-1} (Nicolet MXS, Bruker IFS 113). Spectra of CF_3CSF_3 in Ne and Ar matrices were recorded in the range 2000–200 cm^{-1} (Perkin-Elmer 325, matrix apparatus see ref 6). The liquid phase Raman spectra were measured at −80 °C in the range 2000–50 cm^{-1} with a Coderg T 800 spectrometer and a Kr^+ laser (λ = 647.1 nm, 700 mW, resolution 5 cm^{-1}). Typical spectra are presented in Figure 1, and the experimental frequencies are summarized in Table I.

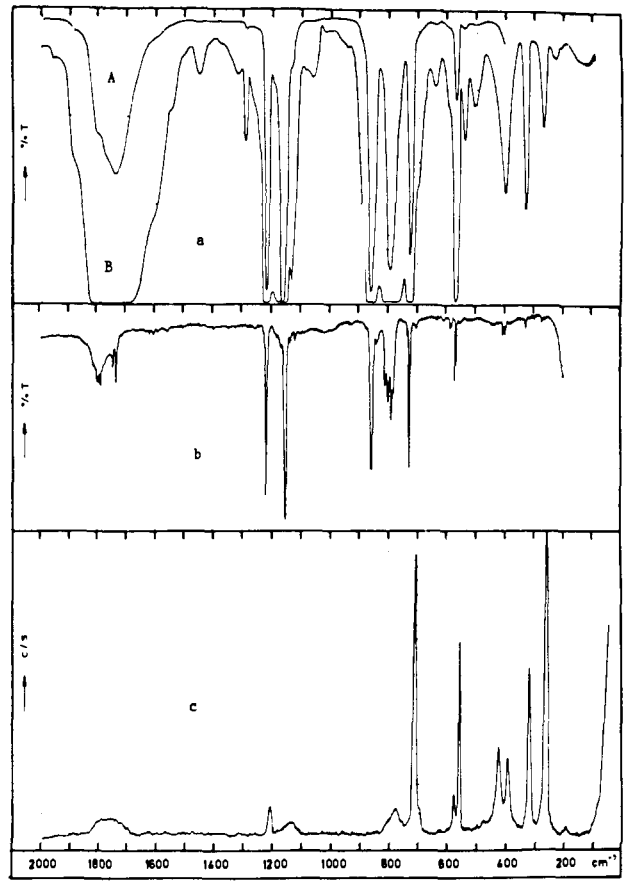

Figure 1. Vibrational spectra: (a) IR gas (10-cm cell with KBr/TPX windows) at 6 (A) and 90 (B) mbar; (b) IR, Ar matrix, 1:1000 at 10 K; (c) Raman, liquid at −80 °C.

Table II. Valence Force Constants[a]

S≡C	12.53	SC/CC	−0.10	CF/FCF	0.32
C—C	5.84	SF/SF	0.22	CF/CCF	0.19
C–F	5.44	SF/SC	0.50	CF/CCF′	−0.17
S—F	4.39	CF/CF	0.87	CC/FCF	−0.25
CCS	0.27	CF/CC	0.34	CC/CCF	0.25
FSF	1.56	SF/FSF	0.35	FSF/FSF	−0.20
CSF	1.58	SF/CSF	−0.29	CSF/CSF	0.33
FCF	1.05	SC/FSF	0.16	FCF/CCF	−0.19
CCF	0.85	SC/CSF	0.61	FCF/CCF′	−0.48

[a] In mydn·$Å^{-1}$, mdyn, and mdyn·Å, respectively.

Electron Diffraction. The scattering intensities were recorded with the Balzers Gasdiffractograph KD-G2[7] at two camera distances (25 and 50 cm) with an accelerating voltage of about 60 kV. Two separate experiments using different samples, which were transported in liquid nitrogen from Berlin to Tübingen, were performed. Due to a very small amount of sample available in the first experiment, only two plates were exposed at each camera distance, whereas four plates were exposed in the second run. The experimental conditions were identical with both runs: sample at −78 °C and stainless steel inlet system and nozzle at room temperature. The camera pressure never exceeded 5.10^{-6} mbar during the experiment, and exposure times were 6–10 and 30–50 s for the long and short camera distance, respectively. The electron wavelength was calibrated by ZnO diffraction patterns. One set of plates from the first run and two sets from the second run were analyzed by the usual procedures.[8] Since no differences between the data of the two runs could be detected, the data were combined for the final structure analyses. The averaged molecular intensities in the s range 1.4–17 and 8–35 $Å^{-1}$ in steps of Δs = 0.2 $Å^{-1}$ are presented in Figure 2.

Microwave Spectroscopy. Broad band microwave spectra were recorded in the X-band microwave region with two different samples by using two different microwave sources: A Marconi A6600 Sweeper,

(5) Dixon, D. E.; Smart, B. E. *J. Am. Chem. Soc.* **1986**, *108*, 2688.
(6) Willner, H. *Z. Anorg. All. Chem.* **1981**, *481*, 117.
(7) Oberhammer, H. *Molecular Structure by Diffraction Methods*; The Chemical Society, Burlington House: London, 1976; Vol. 4, p 24.
(8) Oberhammer, H.; Willner, H.; Gombler, W. *J. Mol. Struct.* **1981**, *70*, 273.

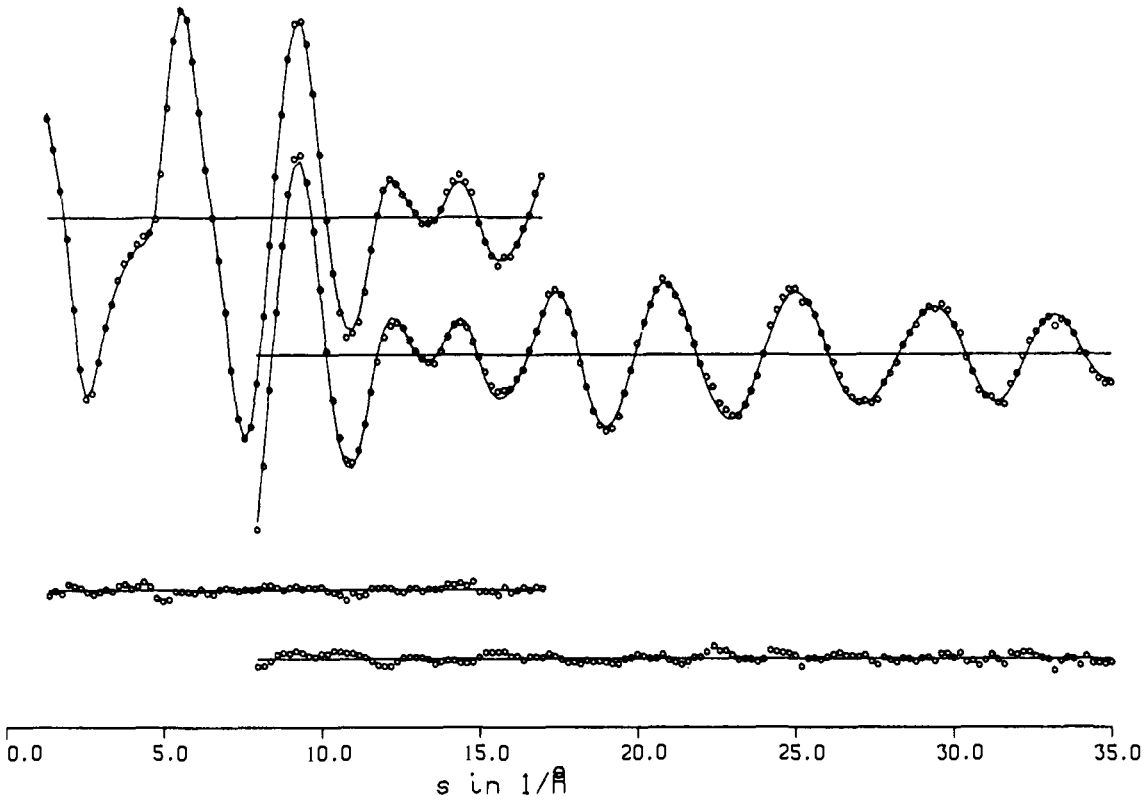

Figure 2. Experimental (●) and calculated (—) modified molecular intensities, sM(s), and differences.

Chart I

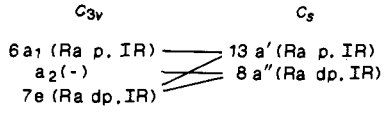

swept by applying a 0–20-V external ramp voltage (effective sweep steps around 3 MHz), and secondly a Gigatronics 900 Microwave synthesizer, driven in 1-MHz steps. In both cases Stark modulation (~1000 V/cm) at 100 kHz was employed. Due to shortage of sample, it was attempted to record the spectra under stationary conditions, but it turned out to be necessary to flow the sample through the cell. Pressures of 0.05 mbar were employed in either case.

Vibrational Assignment and Normal Coordinate Analysis

The distinction between a linear (C_{3v} symmetry) and bent (C_s symmetry) equilibrium structure of CF_3CSF_3 requires a detailed analysis of the vibrational spectra. The assignment of the 21 fundamental vibrations to symmetry species and their correlations are shown in Chart I.

In Figure 1 one can easily distinguish 11 bands in the IR and 12 bands in the Raman spectra. These can all be assigned as fundamentals. This low number of fundamentals leads to an assignment based on C_{3v} symmetry. Possible violations of the C_{3v} symmetry can be modelled in the course of the normal coordinate analysis (see below). The most intensive band in the gas IR spectrum appears around 1800 cm^{-1} and must be assigned as the $\nu_1(a_1)$ C≡S stretching vibration. The extraordinary half-width of this band in all types of spectra can be explained by a hot-band progression ($\nu_1 + n\nu_{14} - n\nu_{14}$, n = 1, 2, 3 ...), similar to that observed for CF_3CN[9] and additional resonating overlap with the combination band $\nu_2 + \nu_5$. The bands at 1800 and 800 cm^{-1} in the Ar and Ne matrices are also broadened due to "matrix effects", such as formation of dimers, distortion in the matrix cage, and association with matrix gas impurities. The two bands near 1200 cm^{-1} are characteristic of CF_3 stretching vibrations. The intensity relationship between IR and Raman spectra prove the symmetric $\nu_2(a_1)$ to lie at higher frequency than the corresponding asymmetric stretch ν_8(e). The stretching vibrations of the SF_3 group are seen in the IR gas spectrum as strong bands at 863 and 795 cm^{-1}. They appear at higher frequencies than the corresponding bands in the NSF_3 spectrum[10] (812 and 768 cm^{-1}). The 863-cm^{-1} band is missing in the Raman spectrum and is assigned as the asymmetric SF_3 stretch ν_9(e) and the weak and broad Raman band at 795 cm^{-1} as the symmetric stretch $\nu_3(a_1)$.

A model calculation using the structural parameters of Table III leads to Δ(PR) = 7.8 cm^{-1} for a_1 bands. Thus, the very intense band at 720 cm^{-1} with a corresponding IR band showing obvious PQR structure must be assigned as $\nu_4(a_1)$. Similarly, the bands at 570 and 330 cm^{-1} are assigned as the symmetric deformations

Table III. Results of Electron Diffraction Analysis (Rigid Model)[a]

(a) Geometric Parameters (r_a Values) in Å and deg

C—F	1.329 (4)	FCF	108.4 (5)
C—C	1.45 (2)	FSF	93.2 (9)
S≡C	1.434 (14)	C—C≡S	155 (3)
S—F	1.561 (3)	tilt (SF_3)	4.8 (21)

(b) Interatomic Distances and Vibrational Amplitudes

C–F	1.33	0.047 (4)	S···F_4	3.29	0.13 (2)
C—C	1.45	0.047[b]	S···F_5	3.62	
S≡C	1.43	0.047[b]	C_2···F_2	3.83	0.17 (7)
S—F	1.56	0.004 (3)	C_2···F_1	4.03	
F_4···F_5	2.15	0.082 (9)	F_2···F_4	3.96	0.14 (3)
F_1···F_2	2.27	0.083 (9)	F_2···F_5	4.36	
C_1···F_4	2.28	0.065[b]	F_1···F_5	4.62	
C_1···F_1	2.57	0.109 (16)	F_1···F_4	4.74	0.13 (3)
C_1···F_2	2.66		F_2···F_6	4.88	
S···C_2	2.81	0.070[b]			

(c) Agreement Factors[c]

R_{50} = 0.040 R_{25} = 0.082

[a] Error limits are 3σ values and include systematic errors due to assumptions for vibrational amplitudes (see text). [b] Not refined. [c] $R = [\sum w_i\Delta_i^2/\sum w_i(s_iM_i(\text{expt}))^2]^{1/2}$, $\Delta_i = s_iM_i(\text{expt}) - s_iM_i(\text{calcd})$.

(9) Faniran, J. A.; Shurvell, H. F. *Spectrochim. Acta A* **1970**, *26A*, 1459.

(10) Müller, A.; Ruoff, A.; Krebs, B.; Glemser, O.; Koch, W. *Spectrochim. Acta A* **1968**, *25A*, 199.

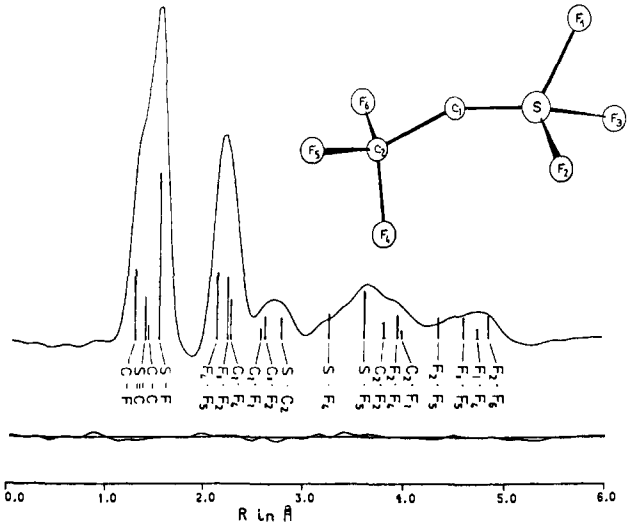

Figure 3. Experimental radial distribution curve and difference curve.

$\nu_5(a_1)$ and $\nu_6(a_1)$. Except for the very weak band around 200 cm^{-1}, seen as well in the IR and Raman, all remaining bands are assigned as e bands. This lowest frequency band is tentatively assigned to $2\nu_{14}$, the overtone of the CCS bending vibration.

For the normal coordinate analysis using the program NORCOR[11] relevant force constants were transferred from CF_3CN,[12] CF_3C-CH,[12] and NSF_3.[13] Interaction force constants were estimated according to ref 14. These force constants were adjusted to fit the experimental frequencies to within 5 cm^{-1}. The force field is shown in Table II. The CCS bending force constant of 0.27 mdyn·Å is typical for linear C—C≡X moieties (0.22 in CF_3—C≡CH,[12] 0.23 in CF_3—C≡N,[12] or 0.28 in *t*-Bu—C≡P[15]) and thus supports the assignment of the 200-cm^{-1} band to the overtone of this bending vibration.

In order to establish a possible deviation of CF_3CSF_3 from C_{3v} symmetry, this force field was used in model calculations with a bent configuration (CCS = 155°). In going from C_{3v} to C_s symmetry all e-type bands split by less than 10 cm^{-1}, except for ν_{10} which splits by 39 cm^{-1}. For the two strongest e-type bands in the matrix IR spectra, ν_8 and ν_9, splittings of 1 and 8 cm^{-1}, respectively, are calculated. These two bands are slightly broader in the matrix spectra (5–8 cm^{-1} half-width) than the corresponding a_1-type bands. The intensities of the remaining e-type bands (ν_{10}–ν_{13}) in the matrix spectra are too low to allow an unambiguous distinction between C_{3v} and C_s symmetry. Additional calculations demonstrate that the splittings of the e-type bands upon bending the C—C≡S skeleton depend on interaction force constants and reduce considerably if some of them are changed slightly. But the orders of magnitude of these splittings are reasonable and are in accordance with recent ab initio calculations.[5] In conclusion, the analysis of the vibrational spectra is most naturally based on a C_{3v} model, but a small deviation from linearity is also compatible with the spectra.

It may be helpful in this context to consider the case of disiloxane, $(SiH_3)_2O$, which is described as "quasi-linear".[16] The vibrationally averaged Si–O–Si angle in disiloxane, measured by electron diffraction, appears to be 144 (1)°.[17] However, most aspects of its vibrational spectra conform to D_{3d} selection rules,[18,19] apparently implying a linear skeleton. Only when isotopic substitution of ^{18}O is used[20] or if the low-frequency gas-phase Raman spectrum is recorded at high resolution,[21] do deviations from D_{3d} behavior become apparent in the vibrational spectra. The detailed analysis in ref 21 leads to an equilibrium Si–O–Si angle of 149 (2)° and a barrier to linearity of only 112 (5) cm^{-1} (1.34 (6) kJ mol^{-1}).

Table IV. Correlation Coefficients with Values Larger Than |0.6|

SC/CC	−0.93	CC/FCF	−0.66
SC/CF	0.70	CC/FSF	0.92
CF/FCF	0.83	$CC/1(F_1\cdots F_2)$	0.62
SC/FSF	−0.83	$SCC/1(C_2\cdots F)$	0.67
SC/FCF	0.69	$FSF/1(F_1\cdots F_2)$	0.63

Structure Analysis

A preliminary analysis of the radial distribution curve (Figure 3) confirms the small FSF angles in the SF_3 group reported by the X-ray[3] and ab initio studies.[4] The radial distribution curve in the range $r > 3$ Å is not compatible with a linear C—C≡S skeleton and can be reproduced only with a C—C≡S angle of about 155°. Such a relatively small deviation from linearity indicates the possibility of a large amplitude C—C≡S bending motion, which in addition to the nearly free rotation of the CF_3 group (ab initio calculations[4] predict a barrier of about 0.15 kJ mol^{-1}) makes the analysis of the experimental intensities rather complicated. Strictly speaking, the bending vibration is a two-dimensional large amplitude motion. Since the simultaneous treatment of all these large amplitude motions would be exceedingly difficult and computationally expensive, three different approximate models were applied in the least-squares analyses: rigid model, model with free internal rotation of the CF_3 group, and model with large amplitude C-C≡S bending motion. In all refinements the experimental intensities were modified by a diagonal weight matrix[8] and scattering amplitudes and phases of J. Haase were used.[22]

In the analysis based on a rigid model C_{3v} symmetry was assumed for CF_3 and SF_3 groups with possible tilt angles between the C_3 axes and the adjacent bonds (C—C or S≡C). Since the tilt angle for the CF_3 group converged toward values which were smaller than their standard deviations, it was set to zero in the ensuing refinements. The C—C and S≡C bond lengths are highly correlated, and their vibrational amplitudes had to be fixed at the spectroscopic values which were calculated from the force field in Table II. Small variations of these amplitudes (±0.003 Å) affected the refined value for the C–C bond length very strongly causing a large uncertainty for this parameter. Other assumptions concerning vibrational amplitudes are evident from Table III. With these constraints eight geometric parameters and nine vibrational amplitudes were refined simultaneously. Correlation coefficients are presented in Table IV. The torsional position of the CF_3 group relative to the SF_3 group has a small effect on the molecular intensities or radial distribution curve. The agreement with experiment is slightly better for the staggered conformation, but the *R* factor for the long camera distance (R_{50}) increases only by 18% for the eclipsed conformation. The refined geometric parameters are nearly equal in both cases except for the SF_3 tilt angle, which is about 4° for the staggered and nearly zero for the eclipsed model and the C—C≡S angle which increases from 155° (staggered) to 157° (eclipsed). The results for the staggered model are summarized in Table III. The SF_3 group is tilted away from the CF_3 group. Error limits are 3σ values and include systematic errors due to the assumptions for C—C and S≡C vibrational amplitudes. A refinement with the C—C≡S skeleton constrained to linearity results in strong increase of the *R* factors (by 120% for R_{50} and 45% for R_{25}), and such

(11) Christen, D. *J. Mol. Struct.* **1978**, *48*, 101.
(12) Galasso, V.; Bigotto, A. *Spectrochim. Acta* **1965**, *21*, 2085.
(13) Königer, F.; Müller, A.; Glemser, O. *J. Mol. Struct.* **1978**, *46*, 29.
(14) Becher, H. J. *Fortschr. Chem. Forsch.* **1968**, *10/1*, 157.
(15) Oberhammer, H.; Becker, G.; Gresser, G. *J. Mol. Struct.* **1981**, *75*, 283.
(16) Thorson, W. R.; Nakagawa, I. *J. Chem. Phys.* **1960**, *33*, 994.
(17) Almenningen, A.; Bastiansen, O.; Ewing, V.; Hedberg, K.; Traetteberg, M. *Acta Chem. Scand.* **1963**, *17*, 2455.
(18) Lord, R. C.; Robinson, D. W.; Schumb, W. C. *J. Am. Chem. Soc.* **1956**, *78*, 1327.
(19) Beattie, I. R.; Gall, M. J. *J. Chem. Soc. A* **1971**, 3569.
(20) McKean, D. C.; Taylor, R.; Woodward, L. A. *Proc. Chem. Soc.* **1959**, 321.
(21) Durig, J. R.; Flanagan, M. J.; Kalasinsky, V. F. *J. Chem. Phys.* **1977**, *66*, 2775.
(22) Haase, J. *Z. Naturforsch. A* **1970**, *25A*, 936.

a linear configuration has to be rejected on the basis of the electron diffraction experiment.

As a next step the effect of internal rotation on the calculated intensities and on the refined values for the geometric parameters was investigated. Assuming free rotation, the geometric parameters change by less than their standard deviations except for the C—C≡S angle, which increases by about 2°, but remains within the error limit given in Table III. The agreement between experiment and model does not improve, and the R factors change by less than 10%. A similar observation has been made earlier in the case of CF_3NCO,[23] where rigid and large amplitude models (free internal rotation) fit the intensities equally well and the CNC angle increases by about 3° for the large amplitude model. For this compound the microwave spectra demonstrate nearly free internal rotation.

In the last step a large amplitude C—C≡S bending motion was introduced into the model. A double-minimum potential of the form

$$V = V_0[(\theta/\theta_0)^2 - 1]^2$$

(θ = 180° − (C—C≡S)), where the barrier to the linear configuration (V_0) and the angle corresponding to the potential minima (θ_0) enter explicitly, was used. Preliminary least-squares analyses demonstrate that V_0, θ_0 and some nonbonded vibrational amplitudes correlate strongly and cannot be refined simultaneously. Furthermore, the Jacobian elements for V_0 are considerably smaller than those of all other parameters. Therefore a large number of refinements with fixed values for V_0 and θ_0 were performed, refining only the parameters listed in Table III except for the SF_3 tilt angle. This parameter was set to zero for the linear configuration and increased by 1° for every 7.5° C—C≡S bending . In some refinements vibrational amplitudes for nonbonded C_2···F and S···F distances converged toward "unreasonably" small or large values and had to be fixed at "reasonable" values. Since the force field does not contain any information about CF_3 torsion, values for these amplitudes cannot be obtained from vibrational spectroscopy. The choice of such "reasonable" values is subjective, and constraining these amplitudes increases the R factor for the long camera distance data (R_{50}) by up to 15% as compared to a refinement where these amplitudes are allowed to converge to "unreasonable" values. Thus, the R factors cannot be used directly as a quantitative criterion for the quality of the fit between experiment and model, and it is not possible to determine a unique minimum in the least-squares analyses. In general, the R factor for the short camera distance data (R_{25}) depends little on the values for V_0 and θ_0, and only the R_{50} will be considered. If we disregard refinements where R_{50} increases by more than 30% relative to the rigid model, we still obtain a number of possible solutions with 25 > V_0 > 2 kJ mol^{-1}. The equilibrium angle θ_0 increases from 25° for V_0 = 25 kJ mol^{-1} (rigid model) to 35° for V_0 = 2 kJ mol^{-1}. It is interesting to note that the average value for the bending angle $\langle\theta\rangle$ = 25 ± 3° for all these possible solutions, corresponding to a $\langle$C—C≡S$\rangle$ angle of 155 (3)°. In all these refinements the geometric parameters are within their error limits equal to those in Table III. If a very broad single-minimum potential corresponding to an average bend of $\langle\theta\rangle$ = 25° is used in the analysis, R_{50} increases by 90%, and the possibility of a linear equilibrium configuration with a very large amplitude bending vibration is not compatible with the electron diffraction experiment.

Microwave Spectroscopy

Molecules possessing low-frequency, large amplitude motions usually exhibit very complicated microwave spectra, which can be very weak due to the unfavorable partition function (see e.g., ref 24 and 25). In the case of heavy molecules the spectra become particularly cumbersome to unravel because of the very small rotational constants. In CF_3CSF_3, therefore (a heavy molecule with a presumably small dipole moment and three large amplitude motions), it seemed out of question to record and analyze the high resolution microwave spectrum in order to derive information on the molecular structure. Instead we chose to record broad band microwave spectra, sweeping the microwave sources rapidly over the lines, thus bunching single absorptions of about the same frequency into aggregates that will show up even in a rapid scan. Molecules most adapted for this kind of spectroscopy are (near-) prolate symmetric tops, whose μ_a-R-branch lines of different excited vibrational states will collapse into single, broad absorptions, appearing every B + C GHz. CF_3CSF_3 is such a molecule.

At first, to preserve sample, broad band spectra were recorded under stationary conditions, only exchanging the gas in the cell approximately every hour. Under these conditions some lines did appear, but the typical μ_a-type R-branch pattern was never observed. Only by flowing the sample through the cell did such a pattern appear—but with the Marconi system, it was only possible to derive very approximate rotational constants, because the frequency of the BWO does not change linearly with the external voltage.

Later on, fortunately, we were able to record another spectrum on a mixture of $CF_3C{\equiv}SF_3$ and $CF_3C(H){=}SF_4$ (the precursor of CF_3CSF_3) by using a Gigatronics 900 synthesizer-sweeper. The most prominent part of this spectrum, however, was not only strong bands, which had also been prominent in the previously recorded spectra of the stationary gas—i.e., these lines originate from the decomposition of CF_3CSF_3, but also a series of "doublets" appeared, whose highest frequency component corresponded to the previously recorded spectrum of pure CF_3CSF_3. In X band, the following absorptions could now be measured accurately: 7.657, 9,202, 10.745, and 12.283 GHz, yielding B + C = 1.545 GHz in very good agreement with the electron diffraction model. (A model with identical bond lengths and angles but possessing a linear back bone has B + C = 1.495 GHz, which is not compatible with the recorded spectrum.) The lower frequency component yields B + C = 1.52 GHz, which fits very well with a reasonable model of $CF_3C(H)SF_4$.

The lines of CF_3CSF_3 have half-widths of approximately 150 MHz. Trial calculations using a torsional-bending-rotation Hamiltonian,[25] showed that this line width would correspond to a bending barrier of approximately 175 cm^{-1} (2 kJ mol^{-1}) and a torsional barrier of about 15 cm^{-1}. Whereas the overall appearance of the spectrum does not seem to be so very sensitive to the height of the torsional barrier, a lowering of the bending barrier (as suggested by the ab initio calculations, see below) will broaden the absorption pattern to a degree which is incompatible with the recorded spectra. The trial calculations, incidentally, also show that large portions of the transitions cannot be resolved by using traditional microwave spectroscopy.

The broad band microwave spectra, which, taken alone, cannot yield a complete molecular structure, strongly support the electron diffraction results, the structural determination as well as the estimate of the barrier to linearity.

Ab Initio Calculations

It is generally found that quantitatively reliable predictions of molecular structures can be obtained from ab initio SCF calculations, provided that the basis set used is of at least double-ζ quality in the valence shell. In addition to this requirement, polarization functions are usually needed on second row atoms. Now calculations of this quality have already been performed for CF_3CSF_3.[4] Since they led to a prediction of a linear C—C≡S skeleton, they are in direct conflict with the electron diffraction results described above. It was therefore clear to us that any further calculations designed to probe the nature of the bending potential in XC≡SF_3 systems would, in order to provide useful, new information, need to go beyond the SCF approach by including electron correlation effects. But in order to obtain an adequate description of electron correlation, the basis set must be far larger than is sufficient for SCF calculations. Since CF_3CSF_3 contains eight "heavy" atoms and one "superheavy" atom, even correlated calculations of the most approximate type

(23) Steger, B. Ph.D. Thesis, Universität Tübingen, 1986.
(24) Nakagawa, J.; Yamada, K.; Bester, M.; Winnewisser, G. *J. Mol. Spectrosc.* **1985**, *110*, 74.
(25) Koput, J. *J. Mol. Spectrosc.* **1984**, *106*, 12.

Table V. Optimized Structural Parameters[a] and Relative Energies[b] for $HCSF_3$ Various Skeletal Bending Angles (DZ(P) Basis)

bending angle	0°	10°	20°	30°	35°	40°	50°	60°
r(C—H)	1.0586	1.0581	1.0589	1.0605	1.0616	1.0630	1.0669	1.0724
r(C≡S)	1.4148	1.4166	1.4221	1.4313	1.4371	1.4437	1.4588	1.4756
r(S—F)[c]	1.5805	1.5830	1.5858	1.5888	1.5903	1.5917	1.59422	1.5961
r(S—F¹)[d]	1.5805	1.5759	1.5705	1.5644	1.5614	1.5585	1.5528	1.5482
∠CSF	124.32	125.39	126.41	127.33	127.76	128.14	128.73	129.08
∠CSF¹	124.32	122.19	119.41	117.84	116.88	115.96	114.48	113.50
∠FSF	91.33	91.27	91.15	90.90	90.71	90.52	90.06	89.54
ΔE, SCF	0.00	0.76	3.07	7.11	9.84	13.11	21.49	33.01
ΔE, MP2	0.00	−0.37	−1.36	−2.54	−2.96	−3.12	−1.75	3.15

[a] Bond lengths in Å, angles in deg. [b] In kJ mol^{-1}. [c] The two F are related by mirror plane. [d] F^1 is in the mirror plane.

Table VI. Optimized Structural Parameters and Relative Energies for $FCSF_3$ at Various Skeletal Bending Angles[a] (DZ(P)Basis)

bending angle	0°	20°	35°	50°	65°
r(C—F)	1.2948	1.2962	1.2998	1.3088	1.3364
r(C≡S)	1.3991	1.4142	1.4493	1.5080	1.5629
r(S—F)	1.5815	1.5897	1.5982	1.6065	1.6074
r(S—F¹)	1.5815	1.5671	1.5537	1.5431	1.5341
∠CSF	124.33	127.80	130.20	132.13	132.05
∠CSF¹	124.33	116.84	111.00	105.80	105.28
∠FSF	91.31	91.09	90.25	88.98	87.57
ΔE, SCF	0.00	2.87	6.98	14.52	36.05
ΔE, MP2	0.00	−6.17	−19.12	−30.98	−12.13

[a] Footnotes as for Table V.

Table VII. Optimized Structural Parameters[a] and Relative Energies[b] for CH_3CSF_3 at Various Skeletal Bending Angles[a] (DZ(P)Basis)

bending angle	0°	10°	20°
r(C—H)[c]	1.0807	1.0807	1.0807
r(C—H¹)[d]	1.0807	1.0807	1.0805
r(C—C)	1.4878	1.4883	1.4918
r(C≡S)	1.4156	1.4175	1.4232
r(S—F)[c]	1.5901	1.5874	1.5852
r(S—F¹)[d]	1.5901	1.5953	1.5993
∠CCH	110.31	110.34	110.39
∠CCH¹	110.31	110.16	110.09
∠HCH	108.62	108.54	108.44
∠CSF	124.76	123.56	122.50
∠CSF¹	124.76	126.95	128.86
∠FSF	90.71	90.70	90.30
ΔE, SCF	0.0	1.82	7.56
ΔE, MP2	0.0	0.22	1.50

[a] Bond lengths in Å, angles in deg. [b] In kJ mol^{-1}. [c] The two H and two F atoms are related by the mirror plane. [d] H^1 and F^1 lie in the mirror plane.

are extremely demanding of computing resources, and unfortunately a realistic correlated mapping of the C-C≡S bending potential in CF_3CSF_3 exceeds our current capabilities.

We, therefore, decided to study three simpler model compounds, $HCSF_3$, $FCSF_3$, and CH_3CSF_3, in some detail. We hoped that they would provide a suitable framework to permit extrapolation to the desired bending potential of CF_3CSF_3. Standard double-ζ basis sets[26] were used (11,7/6,4, 9,5/4,2, and 4/2 for S, C or F, and H) augmented with polarization functions on S and the C atom bonded to S (exponents 0.6 and 0.8). This set, denoted DZ(P), was thought to be a judicious compromise between the requirements for accuracy and realistic computing times. All calculations made use of the program suit GAUSSIAN 82.[27]

Geometries were initially optimized for our three model compounds by SCF gradient methods, assuming linear X-C≡S skeletons (X = H, F, CH_3). Our results are presented in Tables V, VI, and VII and differ only slightly from those reported earlier[4] (for X = H, F) which were obtained by using split-valence bases of 3-21G* (4-21 G) type on S (C, F, H). For CH_3CSF_3 we found the eclipsed conformation to be marginally more stable than the staggered, by just 0.63 kJ mol^{-1}. The other geometrical parameters for eclipsed and staggered conformations were indistinguishable within our convergence limits, which were about 2×10^{-4} Å or 0.03° for bond lengths or angles, corresponding to convergence on the SCF energy of about 5×10^{-7} au (1.3×10^{-3} kJ mol^{-1}) and to convergence on the gradients of 3.0×10^{-4} au. SCF and MP2 energies, at the optimum SCF geometries assuming linear skeletons, are as follows: $HCSF_3$, −734.046519 and −734.661942; $FCSF_3$, −832.861206 and −833.583431; CH_3CSF_3, −773.078576 and −773.780836 au.

Bending potentials were obtained in the following way. With the X-C≡S angle fixed at some suitable nonlinear value, all the remaining geometrical parameters (seven for X = H or F, twelve for X = CH_3) were optimized by SCF gradient methods, imposing C_s symmetry. Results are summarized in Tables V, VI, and VII. For $HCSF_3$ and $FCSF_3$ it was found that the substituent on carbon staggers the SF group, rather than eclipsing it, though the energy

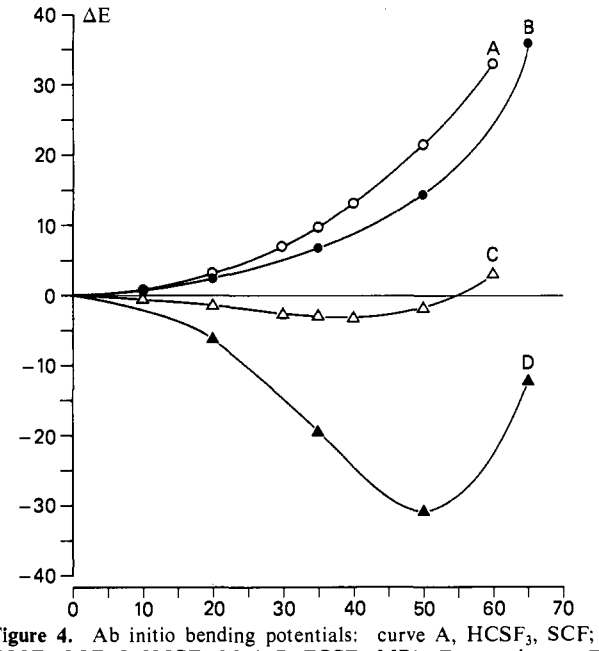

Figure 4. Ab initio bending potentials: curve A, $HCSF_3$, SCF; B, $FCSF_3$, SCF; C, $HCSF_3$, MP2; D, $FCSF_3$, MP2. Energy changes E in kJ mol^{-1}, skeletal bending angle θ = 180 − X—C≡S in deg.

differences between these two conformations are very slight (only 0.51 kJ mol^{-1} for $HCSF_3$ when bent by 20° from linear). At each SCF-optimized geometry, a further calculation was performed incorporating electron correlation, as estimated by second-order Møller–Plesset perturbation theory (MP2).[28] Core orbitals and their virtual counterparts were frozen in the MP2 calculations. Computer-time constraints dictated a rather coarse angular grid

(26) (a) Dunning, T. H.; Hay, P. J. In *Modern* Theoretical *Chemistry*; Schaefer, H. F. Ed.; Plenum Press: New York, 1977; Vol. 3, Chapter 1. (b) Dunning, H. D. *J. Chem. Phys.* **1970**, *53*, 2823.

(27) Brinkley, J. S.; Frisch, M. J.; DeFrees, D. J.; Raghavachari, K.; Whiteside, R. A.; Schlegel, H. B.; Fluder, E. M.; Pople, J. A. Chemistry Department, Carnegie-Mellon University, Pittsburgh, 1983.

(28) Pople, J. A.; Brinkley, J. S. ;Seeger, R. *Int. J. Quantum Chem.* **1976**, *10*, 1.

for the bending potential of $FCSF_3$ (15° spacing between points), as each cycle of geometry optimization required 6 CPU h on a Vax 11/780, while each MP2 calculation required 15 h. Computing times needed for CH_3CSF_3 (for each point) were even greater, but fortunately only two nonlinear points were necessary for this molecule.

We display our bending potentials for $HCSF_3$ and $FCSF_3$ in Figure 4. Three important points are immediately apparent. Firstly, although both molecules are predicted linear at carbon by using SCF wave functions, they are substantially nonlinear once electron correlation is included at the MP2 level. By interpolation we find that $HCSF_3$ is bent by 40° and $FCSF_3$ by 51°. There are very few examples of molecules whose predicted shape is *qualitatively* changed by the inclusion of electron correlation. The only cases known to us prior to this work are $H_2C{=}C{=}C{=}O$,[29] SiC_2,[30] and S_3.[31] Secondly, at both SCF and MP2 levels the bending potentials are rather floppy and unlike those of typical molecules. For $FCSF_3$, the MP2 energy difference between its linear and equilibrium configurations is 31.0 kJ mol^{-1}, whereas to bend CO_2 by 50° requires about 250 kJ mol^{-1};[32] for $HCSF_3$, the MP2 energy difference is only 3.1 kJ mol^{-1}. Finally, we can see from Figure 4 that the MP2 bending potentials of $HCSF_3$ and $FCSF_3$ are quantitatively different, suggesting that it will be difficult to make useful extrapolations to CF_3CSF_3 from model compounds.

The bending potentials for CH_3CSF_3 cannot conveniently be plotted on the same diagram as those of $HCSF_3$ and $FCSF_3$. CH_3CSF_3 has a linear skeleton at the SCF level, but electron correlation once again changes the bending potential substantially. Simple quadratic interpolation between the linear configuration and bends of 10 and 20° lead to an energy minimum at a skeletal bend of just 3°. However, the physical significance of this slight barrier to linearity (of only 0.045 kJ mol^{-1}) is questionable, since the ground vibrational state would presumably lie above such a smaller barrier. On the other hand, we suspect that the MP2 method *underestimates* the relative stabilization of bent forms which is caused by electron correlation, as explained below.

It is clear that electron correlation makes a dramatic difference to the bending potential in all three model compounds described so far. It is therefore unlikely that SCF studies of CF_3CSF_3 will be able to provide quantitatively useful data on the molecular shape or skeletal dynamics. But one may also question whether our MP2 bending potentials are reliable. It is well known that the MP2 method is less than exact, and it has frequently been found to *overestimate* geometrical changes due to correlation.[33]

We, therefore, performed several series of calculations on HC≡SH_3 to explore the effects of improving the level of theoretical rigor associated with our bending potentials.[34] Standard SCF and MP2 potentials for $HCSH_3$ are displayed in Figure 5, as curves G and H. For these standard curves, the same DZ(P) basis and the same optimization procedures were used as for the results presented in Figure 4. Notice that this model compound is substantially nonlinear at carbon even at the SCF level; just as for the XC≡SF_3 systems, however, the bending is increased by using MP2 energies.

In curve I of Figure 5, we show the correlated potential for $HCSH_3$ which results from the DZ(P) basis set and the SCF geometries but using full fourth-order perturbation theory (MP4SDTQ).[35] Evidently at this higher level of theory, the bending is appreciably *more* pronounced than at MP2. Results at intermediate levels (MP3, MP4DQ, and MP4SDQ) differ little

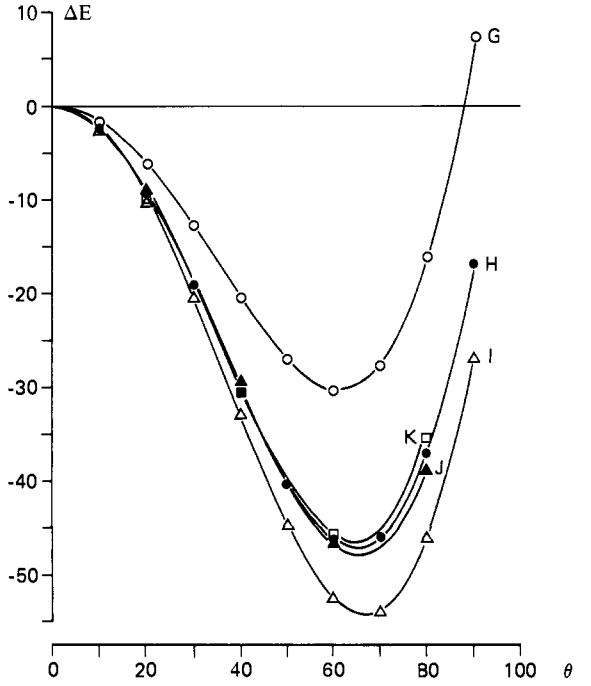

Figure 5. Ab initio bending potentials for $HCSH_3$: curve G, DZ(P), SCF//DZ(P), SCF; H, DZ(P), MP2//DZ(P), SCF; I, DZ(P), MP4//DZ(P), SCF; J, DZP, MP2//DZP SCF; K, DZ(P), MP2//DZ(P), MP2. Energy changes E in kJ mol^{-1}, skeletal bending angle in deg.

from the MP2 values in curve H. Most of the extra fourth-order stabilization on bending arises from the triple substitutions.

We next considered the effects of increasing the size of our basis set, from DZ(P) to DZP, i.e., including polarization functions on all atoms. In curve J we present the bending potential obtained by using DZP MP2 energies at reoptimized DZP SCF geometries. The differences between curves H and J are trivial. Finally we used the original DZ(P) basis but optimized geometries as a function of angle by using MP2 gradient methods rather than the (cheaper) SCF gradient techniques adopted so far. Results are displayed as curve K of Figure 5; notice that for this series of calculations it was necessary to correlate *all* electrons. Differences between H and K are also trivial

These series of calculations have demonstrated that no errors of any consequence are introduced into the bending potentials of $HCSH_3$ if polarization functions are not included on the terminal atoms or if geometries at each point on the surface are optimized by SCF rather then MP2 techniques. However, the degree of bending is *underestimated* by use of MP2 rather than full MP4 theory. To test whether the MP2 underestimation of skeletal bending is unique to HC≡SH_3, we performed a few calculations on FC≡SH_3, equivalent to those reported in curves G, H, and I of Figure 5 for HC≡SH_3.[34] All geometric parameters were optimized, at the DZ(P) SCF level, for the linear skeleton and bending angles of 20° and 40°. $FCSH_3$ is predicted more strongly bent than $HCSH_3$, following the pattern exhibited by $HCSF_3$ and $FCSF_3$, though those three points do not provide sufficient information to yield the optimum skeletal bond angle. Compared to SCF energies, MP2 provides additional lowering of energy on bending through 20° and 40° of 3.5 and 27.4 kJ mol^{-1}, while MP4 yields further lowerings compared to MP2 to 3.8 and 8.6 kJ mol^{-1}. These additional increments due to MP4 over MP2 are several times those found for $HCSH_3$ at the same skeletal angles. We are thus satisfied that MP2 energies underestimate the degree of skeletal bending in XC≡SH_3 systems and see no reason why the same trend should not carry over into XC≡SF_3 systems. Unfortunately, the changes introduced at the MP4 level are almost entirely due to triple substitutions, and the computational requirements to perform full MP4 calculations on even HC≡SF_3 are well beyond our present capabilities.

In the later stages of this work, increased computing power became available to us in Tübingen (Cray 1M and BASF 7/88).

(29) Farrell, L.; Radom, L. *Chem. Phys. Lett.* **1982**, *91*, 373. Brown, R. D.; Dittman, R. D. *Chem. Phys.* **1984**, *83*, 77.
(30) Grev, R. S.; Schaefer, H. F. *J. Chem. Phys.* **1984**, *80*, 3552.
(31) Schaefer, H. F., personal communication to C. J. Marsden, 1986. Burdett, J.; Marsden, C. J., submitted for publication in *J. Am. Chem. Soc.*
(32) Suzuki, I. *J. Mol. Spcetrosc.* **1968**, *25*, 470.
(33) DeFrees, D. J.; Raghavachari, K.; Schlegel, H. B.; Pople, J. A. *J. Am. Chem. Soc.* **1982**, *104*, 5576.
(34) Optimized geometries and energies for the various calculations on $HCSH_3$ and $FCSH_3$ can be obtained from one of the authors (C.J.M.).
(35) Krishnan, R.; Frisch, M. J.; Pople, J. A. *J. Chem. Phys.* **1980**, *72*, 4244.

Table VIII. Optimized Structural Parameters[a] and Relative Energies[b] for CF_3CSF_3 at Various Skeletal Bending Angles

bending angle	3-21*(*) basis									3-21G*(**)	4-31G*
	0°	5°	10°	15°	20°	30°	40°	50°	60°	0°	0°
r(C—F)[c]	1.3163	1.3165	1.3167	1.3168	1.3170	1.3171	1.3175	1.3180	1.3185	1.3205	1.3179
r(C—F¹)[d]	1.3163	1.3161	1.3159	1.3158	1.3153	1.3152	1.3149	1.3146	1.3142	1.3205	1.3179
r(C—C)	1.4645	1.4645	1.4647	1.4647	1.4651	1.4655	1.4664	1.4676	1.4692	1.4627	1.4617
r(C≡S)	1.4089	1.4090	1.4093	1.4098	1.4105	1.4123	1.4149	1.4183	1.4226	1.4132	1.4102
r(S—F)[c]	1.5555	1.5558	1.5562	1.5563	1.5569	1.5575	1.5584	1.5591	1.5596	1.5670	1.5463
r(S—F¹)[d]	1.5555	1.5548	1.5541	1.5536	1.5525	1.5510	1.5491	1.5470	1.5457	1.5670	1.5463
∠CCF	111.36	111.34	111.32	111.31	111.27	111.27	111.25	111.23	111.25	111.16	111.41
∠CCF¹	111.36	111.41	111.45	111.47	111.54	111.60	111.67	111.75	111.75	111.16	111.41
∠FCF	107.53	107.52	107.53	107.52	107.54	107.53	107.53	107.53	107.55	107.73	107.48
∠CSF	123.72	123.92	124.12	124.32	124.52	124.83	125.32	125.69	126.06	123.89	123.56
∠CSF¹	123.72	123.31	122.91	122.47	122.07	121.18	120.32	119.46	118.57	123.89	123.56
∠FSF	92.17	92.16	92.15	92.17	92.17	92.22	92.27	92.36	92.42	91.94	92.43
ΔE, SCF	0.00	0.06	0.25	0.57	1.02	2.36	4.34	7.05	10.56		
ΔE, MP2	0.00	−0.02		0.04	0.27	1.118	2.06				

[a] Bond lengths in Å, angles in deg. [b] In kJ mol^{-1}. [c] The two F on C are related by the mirror plane, as are the two F on S. [d] Both F^1 lie in the mirror plane.

We therefore decided to undertake some calculations on CF_3CSF_3, at both SCF and MP2 levels, though of necessity with use of rather smaller basis sets than were possible for the model compounds already described. The geometry of CF_3CSF_3 was optimized by the SCF gradient methods, for both staggered and eclipsed conformations, initially constraining the skeleton to be linear. A split-valence 3-21G basis[36] was used, augmented with polarization functions on sulfur (exponent 0.65) and both carbon atoms (exponent 0.08). This nonstandard basis is denoted 3-21G*(*). Results are presented in Table VIII for the eclipsed conformation, found to be 0.11 kJ mol^{-1} lower than the staggered. Other geometrical parameters are unchanged, within our convergence limits, by the change in conformation. Our results for bond lengths and angles are naturally close to those already presented by Boggs;[4] the major changes associated with adding polarization functions to carbon are an appreciable shortening of the C–F bonds and a slight lengthening of the nominally single C–C bond.

In Figure 6 we present the SCF and MP2 bending potentials for CF_3CSF_3, obtained with the 3-21G*(*) basis and the procedures already described for the model compounds. At the SCF level, the C-C≡S skeleton is linear but with a very low bending force constant of 0.028 mdyn Å rad^{-2}. Calculations without polarization functions on the carbon atoms[4] predict a much higher C-C≡S bending force constant of 0.2 mdyn Å rad^{-2}.[37] Inclusion of electron correlation using MP2 theory gives a slight skeletal bend of just six degrees away from linear. However, as already mentioned for CH_3CSF_3, the physical significance of the tiny (0.02 kJ mol^{-1}) barrier to linearity indicated by these MP2 calculations is not at all clear.

Two rather larger basis sets were also used to probe the SCF skeletal bending potential in the nearly linear region. Firstly, we augmented the 3-21G basis with two sets of d functions on S (exponents 0.65 and 0.125) and on both C atoms (0.8 and 0.2). Geometrical parameters for the linear skeleton obtained with this nonstandard 3-21G*(**) basis are presented in Table VIII. Changes resulting from the addition of the second, more diffuse set of polarization functions, are mostly slight; rather interestingly, the S–F bond length, which is the most sensitive parameter, actually *increases* by 0.012 Å. Use of this larger basis set reduced the force constant for skeletal bending from 0.028 for 3-21G*(*) to 0.023 mdyn Å rad^{-2}. We also used the 4-31G* basis, containing polarization functions on all atoms, with exponents of 0.65 for S and 0.8 for both C and F. Optimized structural parameters for the linear skeleton are also displayed in Table VIII. Addition of polarization functions to fluorine has produced somewhat shorter S–F bonds, as might be expected, but other changes are trivial. Once again, extension of the basis set lowers the resistance of the skeleton toward bending from 0.028 to 0.022 mdyn Å rad^{-2}.

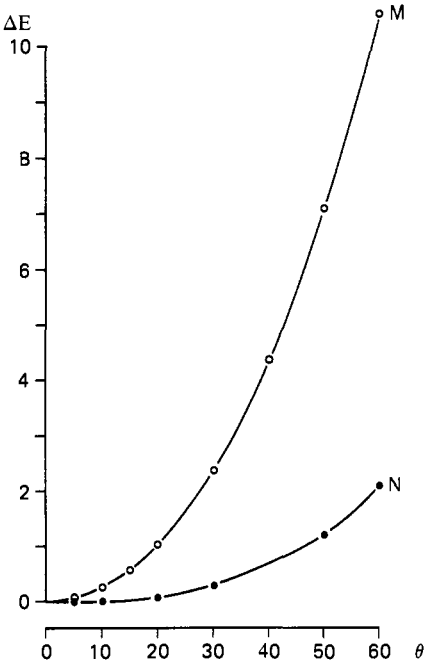

Figure 6. Ab initio bending potentials for CF_3CSF_3 with 3-21G*(*) basis: curve M, SCF; N, MP2. Energy changes E in kJ mol^{-1}, skeletal bending angle in deg.

Results and Discussion

The most striking structural feature of CF_3CSF_3 is the configuration of the C—C≡S skeleton. Independent of the model used, the electron diffraction analysis results in a slightly bent configuration with an "effective" C-C≡S angle of 155 (3)°. This model is in qualitative agreement with the broad band microwave spectra. The IR (gas and matrix) and Raman spectra can most simply be assigned on the basis of a linear configuration with C_{3v} symmetry, but model calculations demonstrate that the spectra are also compatible with a slightly bent C-C≡S skeleton of C_s symmetry of the type indicated by the electron diffraction analysis. This deviation from linearity is more pronounced in the gas phase than in the crystal[3] (171.5 (20)°) and can be rationalized by a small contribution of the ylidic-type resonance structure

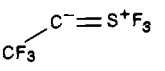

A contribution of this resonance form, which places a formal negative charge on the two-coordinate carbon is supported by computational evidence (the net charges calculated with the 3-21 G*(*) basis are $C^{-0.7}$ $S^{+1.6}$) and experimentally by the surprisingly high field ^{13}C chemical shift of 30 ppm.[3] The increased skeletal bending found in the gas phase compared to the solid should *not*

(36) Binkley, J. S.; Pople, J. A.; Hehre, W. J. *J. Am. Chem. Soc.* **1980**, *102*, 939.
(37) Boggs, J. E., personal communication to H. Oberhammer.

be regarded as an indication that one of the experiments is necessarily flawed. Very little energy is needed to distort the CCS skeleton from 155° to 171°—only a few kJ mol^{-1}—and packing forces in the solid can easily contribute such small amounts. Notice that, in the crystal,[3] the molecules are arranged with their skeletons parallel in adjacent molecules. It is, therefore, plausible that packing could be more efficient for linear skeletons, and the greater deviation from linearity in the gas phase should not be surprising.

Our ab initio calculations on CF_3CSF_3 and on three model compounds $HCSF_3$, $FCSF_3$, and CH_3CSF_3 predict linear X-C≡S skeletons in the SCF-HF approximation, as did earlier work,[4] but we have shown that the inclusion of electron correlation results in bent X-C≡S chains. Similar behavior has been reported for propadienone; HF calculations predict a linear chain, but the incorporation of electron correlation[29] leads to a C=C=C bond angle of about 145°, in excellent agreement with experiment.

In the case of CF_3CSF_3, the skeletal bending predicted by our ab initio calculations is substantially less than that indicated by experimental electron diffraction data. However, CF_3CSF_3 is a fairly large molecule by current ab initio standards, even at the SCF level. We certainly do not claim that our treatment of electron correlation was rigorous or complete; all the indications from our work are that use of larger basis sets and more complete treatment of electron correlation would increase the predicted degree of bending, thereby improving agreement with the electron diffraction experiment. Studies of the bending potentials for $XC{\equiv}SF_3$ systems at the SCF level are likely to be of little quantitative value, as shown by our results in Figures 4 and 6.

Dixon and Smart have very recently reported an ab initio study of CF_3CSF_3,[5] by using a DZ + D(C) basis. They optimized the structure at the SCF level, finding a linear C_{3v} skeleton but with little resistance to bending. They also calculated the vibrational frequencies. As is usual for SCF calculations, their values are too high, by an average of 11%. Their results suggest that ν_3 is higher in frequency than ν_9, the reverse of the assignment made in this work (see Table I) on the basis of Raman intensities. Dixon and Smart also probe the bending potential for CF_3CSF_3 at four skeletal angles by using MP2 energies. The lowest energy is found for a skeletal bend of 171.6° (0.4 kJ mol^{-1} lower than for the linear skeleton), but the energy increases much stronger for larger bending angles (2.2 and 7.1 kJ mol^{-1} for 161.6° and 151.6°, respectively), as indicated by our calculations (see Figure 6 or Table VIII). This strong increase in energy is at least partly due to the fact that the remaining 12 geometric parameters have not been optimized at bending angles 161.6 and 151.6°. Qualitatively, these results are in agreement with our calculations, in that inclusion of electron correlation in the MP2 approximation shifts the energy minimum from linear to a slightly bent skeletal configuration.

Although the electron diffraction experiment shows unequivocally that the effective C-C≡S angle in CF_3CSF_3 is close to 155°, it does not provide information on the dynamics of the bending motion, except for an estimate for the lower limit of the barrier to linearity (2 kJ mol^{-1}). Unfortunately, the corresponding vibration has not been observed in either the IR or Raman spectra. Although the assignment of the 200-cm^{-1} band to the overtone of this vibration results in a reasonable value for such a force constant, it is not definitive. If this assignment is correct, a unique solution can be selected among the various large-amplitude models which are compatible with the electron diffraction data. A double-minimum potential with a barrier of 3.5 kJ mol^{-1} and an equilibrium C-C≡S angle of 150° leads to the same value for the bending force constant as derived from the vibrational data. This value is somewhat larger than that estimated from the microwave data (2 kJ mol^{-1}) but considering the approximations involved (shape of the potential, harmonic vibration, etc.), the agreement is reasonably good. We stress, however, that a more refined treatment of the dynamics of this motion based on high resolution spectra, for example, using a "semirigid bender" model,[38] might change somewhat the numerical values we suggest here.

With the exception of the C-C≡S angle, the geometric parameters derived from the electron diffraction experiment (see Table III) are in good agreement with the crystal values,[3] if the latter are corrected for anisotropic vibrational motion. The C≡S bond length of 1.434 (14) Å (1.420 (5) Å in the crystal) is extremely short, as has been discussed previously.[3] The S-F bond distances of 1.561 (3) Å (1.568 Å in the crystal) are indistinguishable from those in SF_6 (1.5620 (2) Å).[39] The gas-phase value for the C-F bond lengths of 1.329 (4) Å are very similar to those in other CF_3 groups bonded to sp-hybridized carbon atoms, such as CF_3CCCF_3 (1.331 (2) Å)[40] or CF_3CN (1.335 (10) Å).[41] The corresponding values in the crystal[3] (1.360 Å) are rather longer; the correction due to thermal motion is substantial for these distances, on account of the torsional vibration about the CF_3-C bond. Ab initio values for the C-F bond length are moderately sensitive to details of the basis, being shortened when d functions are included on the carbon atom. Our 3-21G*(*) set predicts 1.316 Å, Dixon and Smart's DZ + D(C) basis[5] gives 1.323 Å, and the 4-21G set[4] predicts 1.360 Å. It has been shown that unpolarized bases of the 4-21G type systematically overestimate C-F bond lengths by about 0.03–0.04 Å.[42] FSF angles from the various structural studies are in excellent agreement; 93.2 (9)° in the gas, 93.0 (average value) in the crystal,[3] and 92.2, 92.3[5] or 92.7[4] from the three sets of ab initio calculations.

Prior to this work, relatively few cases were known of nonlinear coordination at formally sp-hybridized carbon atoms. All such examples involved cumulated double bonds, as in propadienone,[29] $H_2C{=}C{=}C{=}O$, or $Ph_3P{=}C{=}PPh_3$.[43] Our work suggests that such nonlinear coordination may occur rather more widely than has hitherto been suspected. In addition to the examples containing $C{\equiv}SF_3$ bonds discussed in this paper, our preliminary ab initio results[44] predict that $HC{\equiv}PF_2$ is also nonlinear at carbon, even at the SCF level.

Conclusion

Analyses of the electron diffraction intensities using rigid or nonrigid molecular models result in a nonlinear C—C≡S skeleton in CF_3CSF_3, with an average C-C≡S angle of 155 (3)°. The microwave rotational constants confirm this model, whereas IR matrix spectra are compatible with linear as well as slightly bent models. The barrier to linearity is estimated to be ≥2 kJ mol^{-1} from electron diffraction and microwave data. Ab initio calculations for model compounds and for CF_3CSF_3 result in nonlinear skeletons only if electron correlation is included. Although the predicted degree of bending in CF_3CSF_3 is much smaller than that derived from experiment, our calculations indicate that the use of larger basis sets and more complete treatment of electron correlation would improve the agreement.

Acknowledgment. H.O., K.S., and H.W. thank the Fonds der Chemischen Industrie for financial support. C.J.M. thanks Melbourne University Computing Service for access to substantial computer time. D.C. thanks Fa. KONTRON for putting a Gigatronic 900 synthesizer at our disposal for recording of part of the microwave spectrum.

Note Added in Proof. After submission of this paper further increased computing power became available to us which allowed calculations for $CF_3C{\equiv}SF_3$ at higher levels of electron correlation (MP3, MP4SD, and MP4SDQ). Calculations were performed for CCS angles between 180° and 120° at the HF/3-21G*(*) optimized geometries (Table VIII) with the same basis set. With

(38) Bunker, P. R.; Landsberg, B. M. *J. Mol. Spectrosc.* **1977**, *67*, 374.
(39) Holder, C. H.; Gregory, D.; Fink, M. *J. Chem. Phys.* **1981**, *75*, 5318.
(40) Kveseth, K.; Seip, H. M.; Stolevik, R. *Acta Chem. Scand.* **1971**, *25*, 2975.
(41) Thomas, L. F.; Heeks, J. S.; Sheridan, J. *Z. Elektochem.* **1957**, *61*, 935.
(42) See, e.g.: Christen, D.; Ramme, K.; Haas, B.; Oberhammer, H.; Lentz, D. *J. Chem. Phys.* **1984**, *80*, 4020.
(43) Vincent, A. T.; Wheatley, P. J. *J. Chem. Soc., Dalton Trans* **1972**, 617.
(44) Marsden, C. J., research in progress.

increasing level of theory the position of the energy minimum shifts from 180° (HF) to 145° (MP3), 140° (MP4SD), and 130° (MP4SDQ), and the energy relative to the linear configuration decreases by 0.28 (MP3), 0.54 (MP4SD), and 0.92 (MP4SDQ) kJ·mol^{-1}. These calculations thus confirm the ab initio results for the model compounds $HCSH_3$ and $FCSH_3$, in that higher levels of electron correlation increase the degree of bending, and definitely result in a bent equilibrium configuration of the C—C≡S skeleton in $CF_3C{\equiv}SF_3$, in agreement with the experimental data.

Comparison of Structure and Thermal Chemistry of Stoichiometric and Catalytic Alkoxy-Substituted Molybdenum Heteropolyanions: ^{13}C CP-MAS NMR Spectrum of a Chemisorbed Reaction Intermediate

W. E. Farneth,* R. H. Staley, P. J. Domaille, and R. D. Farlee

Contribution from E. I. du Pont de Nemours and Co., Central Research and Development Department, Experimental Station, Wilmington, Delaware 19898. *Received October 27, 1986*

Abstract: This paper reports the spectral and chemical properties of methanol chemisorbed on $K_{3-x}H_xPMo_{12}O_{40}$. The heterogeneous gas/solid reaction was investigated by a variety of techniques including the following: vacuum gravimetric measurements, temperature-programmed desorption, infrared spectroscopy, solid-state ^{13}C CP-MAS NMR, and comparison with stoichiometric model compounds. It is demonstrated that residual proton content in the heteropolyanion (HPA) salt plays an important role in the generation of reactive, chemisorbed intermediates. A methoxy group that occupies a bridging site in the HPA lattice is shown to be a key intermediate on the pathway to both dehydration and oxidation products. The structure of the methoxy intermediate is confirmed by spectral comparison with an identical, methylated Keggin anion salt of known structure.

Heteropolyacids and their salts occupy an interesting intermediate structural position between solid state metal oxides and small mono- or bimetallic coordination compounds. They are discrete molecular clusters containing 6, 12, or larger numbers of metal atoms linked through oxide bridges.[1] Because they are discrete molecular systems they are easier to characterize and rationally modify than the surfaces of metal oxide solids. Their chemistry and spectroscopy therefore offer great promise as a model for heterogeneous metal oxide catalyst systems. In addition, many heteropolyanion systems are interesting as catalytic materials in their own right.[2] The confluence of these two incentives has led to a growing effort to understand the electronic structure, spectra, and chemistry of these compounds, particularly the best known class of $XM_{12}O_{40}$ compounds having the so-called Keggin structure. In this paper we report the spectral and chemical properties of methanol chemisorbed on $K_{3-x}H_xPMo_{12}O_{40}$ and an alkylated analogue of this heteropolyanion, $Cs_2(OCH_3)PMo_{12}O_{39}$. We demonstrate that (1) residual proton content in the heteropolyanion salt plays an important role in the mechanism of alcohol oxidation over these materials, (2) a methoxy intermediate is formed on the heteropolyanion surface during chemisorption, (3) the surface methoxy formed by dissociative chemisorption of methanol is spectroscopically and chemically similar to that formed by direct alkylation in solution and, therefore, probably occupies a bridging site in the HPA skeleton, and (4) this intermediate can be involved in a redox cycle that leads to "O" atom loss from the HPA. The adsorbed methoxy described in this paper is one of only a handful of chemisorbed heterogeneous reaction intermediates that has been directly observed by solid-state NMR.

Experimental Section

$K_{3-x}H_xPMo_{12}O_{40}$ was prepared by precipitation from a solution of $H_3PMo_{12}O_{40}{\cdot}nH_2O$ and K_2CO_3 in H_2O. The components were added in a molar ratio of 2/3 at $n = 30$.[4] The precipitate was filtered, washed with distilled water, and dried. The material is a bright yellow, polycrystalline powder. Electron microscopy shows it to consist of roughly spherical particles of 0.2-1.0-μm diameters, with prominent surface irregularities. Although literature would suggest that this is a preparation procedure for $K_3PMo_{12}O_{40}$, the elemental analysis data, and especially the chemistry and spectroscopy (vide infra), make it clear that $K_{3-x}H_xPMo_{12}O_{40}$ is a better representation of the molecular formula for this material. Elemental analyses were obtained from Mikroanalytisches Labor Pascher, Bonn, West Germany. Calcd for $K_3PMo_{12}O_{40}{\cdot}5H_2O$: K, 5.78; P, 1.53; Mo, 56.73; O, 35.48; H, 0.49. Found: K, 4.85; P, 1.60; Mo, 58.30; O, 34.60; H, 0.48. The BET surface area is ~60 m^2/g, in reasonable accord with previous reports, and indicative of significant porosity in these particles. Goodenough et al. have recently shown that solid-state ^{31}P NMR and X-ray diffraction are both capable of detecting the presence of a discrete $H_3PMo_{12}O_{40}$ phase in $K_3PMo_{12}O_{40}{\cdot}5H_2O$ samples.[5] The ^{31}P solid state NMR (Nicolet NT-360, operating at 146.095 MHz with magic-angle spinning) of this sample is very clean. Only a single sharp peak at −3.9 ppm (fwhm = 0.5 ppm) relative to external 85% orthophosphoric acid is observed. Similarly, the X-ray powder pattern (2θ = 2–60°, Philips APD-3600) is identical with that previously reported for $K_3PMo_{12}O_{40}$ and shows no additional features that could be associated with a discrete H_3 phase.[5]

^{13}C magic-angle spinning (MAS) spectra were obtained on both a General Electric S-100 spectrometer (25.2 MHz) and a Bruker CXP-300 spectrometer (75.5 MHz). Dry nitrogen gas was used to drive MAS at rates of 2.5 kHz (S-100) to 4 kHz (CXP-300). The magic angle was set by minimizing the line width of the side bands of the Br-79 satellite transitions in KBr.[6] The Hartmann–Hahn matching condition for

(1) Pope, M. T. *Heteropoly and Isopoly Oxometalates*; Springer-Verlag: Berlin, 1983.

(2) (a) Misono, M. In *Catalysis by Acids and Bases*; Imelik, B. et al. Eds.; Elsevier: Amsterdam, 1985; p 147. (b) Renneke, R.; Hill, C. L. *J. Am. Chem. Soc.* **1986**, *108*, 3528.

(3) See Finke et al. (Finke, R. G.; Rapko, B.; Saxton, R. J.; Domaille, P. J. *J. Am. Chem. Soc.* **1986**, *108*, 2947) for a thorough discussion of the problems in preparation and characterization of these types of compounds.

(4) Tsigdinos, G. A. *Ind. Eng. Chem. Prod. Res. Dev.* **1974**, *13*, 267. n = 30 was established from TGA data.

(5) Black, J. B.; Clayden, N. J.; Gai, P. L.; Scott, J. D.; Serwicka, E.; Goodenough, J. B. *J. Catal.*, in press.

(6) Frye, J. S.; Maciel, G. E. *J. Magn. Reson.* **1982**, *48*, 125.

0002-7863/87/1509-4018$01.50/0